Charles University in Prague

The First Faculty of Medicine

Summary of Doctoral Thesis

UNIVERZITA KARLOVA
1. lékařská fakulta

Alternative methods for visualization of pancreatic islets

Mgr. Andrea Gálisová

2018

Doctoral studies in biomedicine

Charles University in Prague and the Academy of Sciences of the Czech Republic

Study program:	Medical Biophysics
Board chairperson:	Prof. MUDr. RNDr. Jiří Beneš, CSc.
Training workplace:	MR Unit, Department of Diagnostic and Interventional Radiology Institute for Clinical and Experimental Medicine in Prague
Thesis Supervisor:	Doc. Ing. Daniel Jirák, PhD.
Thesis Consultant:	Mgr. Vít Herynek, PhD.

Content

Abstract

Transplantation of pancreatic islets (PIs) represents an alternative treatment for type 1 diabetes mellitus. Post-transplant monitoring of islets by a reliable imaging method may contribute to the improvement of the transplantation outcome. In this thesis, novel visualization approaches for PIs were tested using magnetic resonance (MR) and optical imaging on phantoms and experimental animals, including Chemical Exchange Saturation Transfer (CEST) MR, fluorine (^{19}F) MR, bioluminescence and fluorescence imaging.

MR imaging based on frequency-selective method CEST was performed on islets labeled with Eu-/Yb-based chelates. Labeled islets possessed low MR signal in phantoms, what would have been unsatisfactory for *in vivo* applications. Moreover, viability and function of labeled islets was impaired reflecting limited applicability of these agents for islet labeling and visualization.

Genetically modified bioluminescent islets showed suitable properties for longitudinal tracking of their post-transplant fate at an artificial transplant site - subcutaneously implanted polymeric scaffolds. Using multimodal imaging (MR and bioluminescence), the optimal timing for transplantation of islets into the scaffolds was assessed in diabetic rats. Islets transplanted into scaffolds using the optimized timing scheme were sufficiently vascularized and functional.

Finally, we developed a trimodal imaging platform for islets transplanted into polymeric scaffolds in rats. Bioluminescent islets labeled with multimodal nanoparticles were specifically visualized by ^{19}F MR and sensitively by fluorescence imaging. A correlation between the bioluminescence and the ^{19}F MR signals was found indicating the fast clearance of nanoparticles from the transplantation site after cell death. This finding addresses one of the major issues with intracellular imaging labels and proved that the proposed imaging model is reliable for reflecting the status of transplanted PIs *in vivo*.

Keywords: magnetic resonance imaging, optical imaging, contrast agents, cell labeling, pancreatic islet, transplantation

Abstrakt

Transplantace pankreatických ostrůvků (PIs) představuje alternativní metodu léčby diabetu 1. typu. Monitorování transplantovaných PIs pomocí vhodné zobrazovací metody může přispět k zlepšení výsledků transplantace. V předkládané disertační práci jsme testovali nové způsoby zobrazení PIs pomocí magnetické rezonance (MR) a optického zobrazování, konkrétně MR metodu založenou na přenosu saturace magnetizace přes chemickou výměnu (Chemical Exchange Saturation Transfer - CEST), fluorovou (^{19}F) MR a optické zobrazování.

Frekvenčně selektivní CEST metoda byla použita pro zobrazování PIs značených pomocí dvou CEST kontrastů. Na MR obrazech jsme detekovali pouze slabý signál ze značených ostrůvků, které byly navíc poškozené. Tyto výsledky ukazují, že tento typ kontrastů není vhodný pro značení a zobrazování pankreatických ostrůvků.

V druhém experimentu jsme monitorovali geneticky modifikované bioluminiscenční ostrůvky transplantované do arteficiálních skeletů implantovaných do podkoží, které představují alternativní transplantační místo. Multimodálním zobrazováním (MR a bioluminiscence) jsme určili optimální časování transplantačních kroků. Ostrůvky transplantované diabetickým potkanům podle optimalizovaného protokolu byly dostatečně prokrvené a funkční.

Vyvinuli jsme také nový trimodální zobrazovací model pro PIs transplantované ve skeletech. Značené bioluminiscenční ostrůvky byly zobrazené pomocí specifického ^{19}F MR zobrazování a senzitivního fluorescenčního zobrazování. Důležitým výsledkem je korelace ^{19}F MR a bioluminiscenčního signálu, která ukazuje, že po destrukci PIs jsou nanočástice z transplantačního místa odstraněna a proto nepřispívají k falešně pozitivním výsledkům. Experimenty potvrdili, že navrhovaný zobrazovací model je vhodný pro sledování transplantovaných ostrůvků *in vivo*.

Klíčová slova: magnetická rezonance, optické zobrazování, kontrastní látky, buněčné značení, pankreatické ostrůvky, transplantace

1 Introduction

Non-invasive imaging represents an efficient diagnostic tool in medicine and it can be found in many areas including cellular imaging. Part of this hot topic area is imaging of pancreatic islets (PIs) both in experimental and clinical practice. There are many imaging options for PIs visualization, from which magnetic resonance (MR) and optical imaging belong to one of the most advantageous methods. In this thesis, we investigated alternative imaging approaches based on these two imaging methods and we applied them on visualization of transplanted PIs.

1.1 Transplantation of pancreatic islets

Transplantation (Tx) of PIs represents an alternative treatment for type 1 diabetes mellitus (Shapiro et al. 2006). Islets are usually transplanted into the liver; however, this method has several limitations and it is accompanied by a massive destruction of the transplanted grafts. To overcome these limitations, extrahepatic transplantation sites are being tested. Subcutaneously implanted macroporous scaffolds showed promising properties by providing an easy access, minimally invasive surgery and a possibility of removal in case of complications and are suitable for monitoring by imaging methods.

1.2 Visualization of pancreatic islets

To elucidate the processes of islet engraftment and rejection, the use of imaging methods is of a great help. Precise monitoring of islet viability, distribution and mass by a reliable method could contribute to improvement of transplantation outcomes and optimization of transplantation protocols. Visualization of transplanted PIs is conditioned by their labeling with contrast agents or by genetic engineering of islets in order to create contrast between the islets and the host tissue. Each imaging method provides different information and

is accompanied by various limitations as low spatial resolution (radionuclide imaging), low specificity (proton (^{1}H) MR), low sensitivity (fluorine (^{19}F) MRI) or signal attenuation (optical methods). The most widely used agents for islet labeling are superparamagnetic iron oxides nanoparticles (SPIONs) used for ^{1}H MRI (Jirák et al. 2004). On the other hand, highly sensitive SPIONs offer low imaging specificity (due to other sources of hypointense MR signal in tissues) and enable only relative quantification of islet number. Due to the lack of proper contrast agents for transplanted PIs, this thesis aimed to test alternative probes and approaches for imaging of transplanted PIs. Novel contrast agents for MRI (based on chemical exchange saturation transfer (CEST) and fluorine-containing probes for ^{19}F MRI) and fluorescence imaging were tested, as well as genetically modified cells trackable by bioluminescence imaging.

1.3 Alternative labels for pancreatic islets

1.3.1 Chemical exchange saturation transfer

CEST imaging allows frequency-selective saturation of exchangeable protons in a compound and thus a possibility of simultaneous visualization of various CEST agents/labeled cells or islets in one MR experiment (Ward et al. 2000). CEST contrast is dependent on various intrinsic parameters (e.g. pH and temperature) and can be switched on and off. This approach has been applied in a variety of application; however not yet for visualization of labeled pancreatic islets.

1.3.2 Bioluminescence and fluorescence imaging

Bioluminescence imaging is based on oxygenation of luciferins in a biochemical reaction catalyzed by enzyme luciferase, which produces light. Bioluminescence provides specific tracking of genetically modified cells with expression of luciferase. An advantage of bioluminescence is visualization of only viable cells (Kim et al. 2015).

Fluorescence provides a sensitive detection of fluorescent probes after excitation at a specific frequency. For *in vivo* applications, the near-infrared probes are preferred due to low absorption in the biological tissues.

1.3.3 Fluorine (^{19}F) MRI

The main advantage of using ^{19}F isotopes as MR contrast agents to ^{1}H is their negligible natural content in the tissues, what leads to high specificity of visualization (Srinivas et al. 2012). ^{19}F MR allows absolute quantification of ^{19}F atoms, which enables estimation of the number of cells labeled with fluorine-containing probes. The drawback of ^{19}F MR is low sensitivity due to low amount of ^{19}F per a molecule of a synthetized agent; therefore compounds with high number of ^{19}F atoms are needed.

1.3.4 Multimodal imaging

Multimodal imaging represents a future perspective for molecular imaging by providing more complex information about transplanted cells.

Using bioluminescence and MR, viability and vascularization of transplanted cells can be assessed, what can contribute to optimization of transplantation protocol (e.g. in artificial scaffolds).

Moreover, combining specific ^{19}F MR and sensitive optical imaging (bioluminescence and fluorescence) methods can provide complementary information about islet distribution and *in vivo* viability of transplanted islets.

2 Aims

The aim of the proposed thesis is pre-clinical examination and validation of alternative visualization approaches for pancreatic islets by MR and optical imaging. Feasibility of the novel contrast mechanisms is tested in order to improve detection of the transplanted graft and enhance the transplantation outcome. The specific aims are following:

1) Testing of frequency-selective MR contrast agents based on CEST effect for labeling of pancreatic islets.
The aim is to test the feasibility of visualization of pancreatic islets labeled by CEST agents.

2) Visualization of pancreatic islets by bioluminescence imaging.
The second aim of the thesis is to implement bioluminescence for long-term *in vivo* tracking of localization and viability of transplanted islets at alternative transplant site (polymeric scaffolds). The purpose of this study is optimization of the transplantation protocol in the scaffolds using a multimodal approach (MRI and bioluminescence).

3) Trimodal imaging of pancreatic islets labeled with multimodal nanoparticles using ^{19}F MR and optical imaging.
The third task is optimization of labeling of pancreatic islets with multimodal nanoparticles that are trackable by ^{19}F MR and fluorescence imaging. Optimized labeling route should be implemented for longitudinal multimodal *in vivo* visualization (^{19}F MRI, fluorescence, bioluminescence) of pancreatic islets transplanted in artificial scaffolds.

3 CEST agents for labeling of pancreatic islets

3.1 Materials and Methods

Two paramagnetic chelates containing europium (Eu-DO3A-ae) or ytterbium (Yb-DO3A-ae) were tested by CEST imaging on a 4.7 T MR scanner.

Isolated rat pancreatic islets were labeled with various concentrations of the agents (45 – 100 mM) by pinocytosis (incubation in a culture medium within 12 or 24 hours) and microporation (application of electric pulses with 600 – 1000 V). Viability of islets was assessed with propidium iodide and acridine orange, insulin secretion was measured after stimulation with glucose and intracellular uptake of the agents in islets was assessed by inductively coupled quadrupole plasma mass spectrometry (ICP-QMS).

Labeled islets (200 – 1000 islets) were washed and placed in a phantom (gelatin or buffer) and measured by *in vitro* CEST imaging using the parameters: repetition time TR = 5000 ms, echo time TE = 8.9 ms, spatial resolution 0.43 × 0.43 × 2 mm^3. A pre-saturation pulse (2000 ms/ 35 μT) was applied at the specific frequencies: 19 ppm and 34 ppm for Eu-DO3A-ae; 42 ppm and 89 ppm for Yb-DO3A-ae.

Alternatively the whole Z-spectrum was acquired by saturation at -110 ppm to +110 ppm (step 2.5 ppm; a saturation pulse 2000 ms/ 35 μT). WAter Saturation Shift Referencing (WASSR) correction was accomplished by direct water saturation with higher frequency resolution ranging from -1.5 ppm to +1.5 ppm (step 0.25 ppm, a saturation pulse 100 ms/0.5 μT).

CEST effect was expressed as asymmetric magnetic transfer ratio (MTR_{ASYM}) and calculated from a region of interest (ROI) on the pixel wise basis according to the formula

$$MTR_{ASYM} = \frac{S_{SAT}(\Delta\omega)}{S_{SAT}(-\Delta\omega)} * 100\%, \quad (1)$$

where $S_{SAT}(\Delta\omega)$ and $S_{SAT}(-\Delta\omega)$ are water signal intensity after saturation at the frequency offsets $\Delta\omega$ and $-\Delta\omega$, respectively.

3.2 Results and Discussion

CEST imaging revealed higher MTR_{ASYM} values of Eu-DO3A-ae compared to Yb-DO3A. Labeling by pinocytosis was more efficient than microporation. The intracellular uptake of the agents after pinocytosis reached the detection threshold, in contrast to microporation that did not lead to sufficient uptake.

CEST MRI experiment proved **feasibility of *in vitro* visualization** of PIs labeled by Eu-DO3A-ae and Yb-DO3A-ae chelates using pinocytosis; however with the drawback of **viability and functionality impairment**. Islets labeled with 100 mM of Eu-DO3A-ae were successfully detected *in vitro* with 20% MTR_{ASYM} signal, whereas islets labeled with 100 mM of Yb-DO3A-ae reached only 4% of MTR_{ASYM}. Islets labeled with 80 mM of Eu-DO3A-ae provided about 8% MTR_{ASYM} and the islets labeled with 80 mM of Yb-DO3A-ae were not detected. Islets labeled with 60 mM were detected after correction of $\boldsymbol{B_0}$ inhomogeneites (WASSR approach) with MTR_{ASYM} around 5% (Fig. 1).

However, higher CEST effect was detected from islets labeled with higher agent concentration, viability of the labeled islets was low; using concentration above 60 mM for 24-hour incubation, viability of islets decreased below 70% and insulin secretion was impaired. Islet viability above 80% was reached using shorter incubation time (12 hours) and concentrations below 40 mM, which was not sufficient for detection of the CEST effect. Islets labeled by pinocytosis for longer time (leading to higher uptake of the complexes in PIs) expressed lower viability probably due to a slow release of **a toxic lanthanide ion** under acidic condition (pH<6) as has been already reported (Krchová et al. 2013). We propose that the same effect occurred in endosomes (lysosomes) during pinocytosis in our study.

Importantly, our findings of **low sensitivity of CEST imaging** for cellular imaging corresponded to the published data. A recent report at 9.4T showed *in vitro* CEST signal from labeled cells around 1.1% or 12% for Eu- and Yb-labeled cells, respectively (Nicholls et al. 2015).

In summary, the decrease of CEST effect in endosomes after labeling by pinocytosis together with deterioration of islet viability after labeling by higher concentration of the agents and low CEST signal originating from PIs labeled at low concentration, make the CEST agents at current experimental setting unsuitable for *in vivo* application in PIs labeling and visualization.

The data were published in two publications in impacted journals (Gálisová et al. 2016; Krchová et al. 2016).

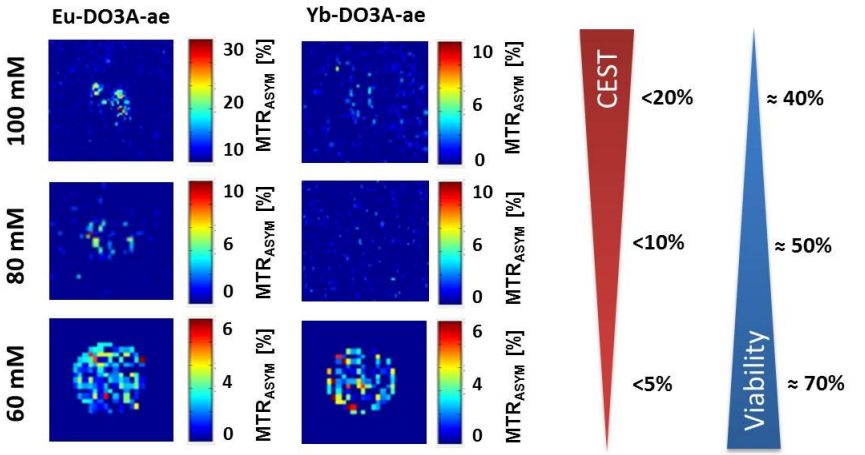

Fig. 1. Visualization of pancreatic islets labeled with CEST agents. Islets labeled with Eu-DO3A-ae provided higher MTR_{ASYM} values. Higher CEST signal was detected from islets labeled with higher concentration of CEST agents; however viability was impaired at high concentrations.

4 Bioluminescence imaging of transplanted pancreatic islets

4.1 Materials and Methods

Subcutaneously implanted artificial macroporous scaffolds served as an alternative transplantation site for PIs. The scaffolds were supplemented with rods for creation of a cavity for transplanted cells. The scheme of transplantation steps is shown in Fig. 2.

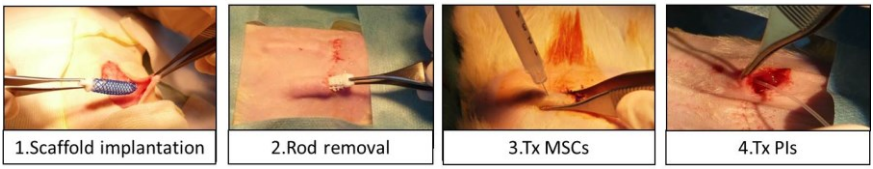

Fig. 2. A scheme of transplantation steps. Firstly, a scaffold supplemented with a rod is implanted subcutaneously in the abdominal part of an animal (A). One week after scaffold implantation, the rod is removed (B). Transplantation of mesenchymal stem cells (Tx MSCs) is performed immediately after the rod removal (C) or the scaffold is left empty (with NaCl). The last step is transplantation of pancreatic islets (Tx PIs) (D) on day 4 or 7 after the rod removal.

Because adequate vascularization is crucial for survival and long-term function of transplanted islets (especially in the poor-vascularized scaffolds), mesenchymal stem cells (MSCs) with angiogenic potential were transplanted in the scaffolds prior PIs.

The effect of bioluminescent MSCs on vascularization in scaffolds was examined using multimodal imaging in healthy Lewis rats (n=6). Perfusion and vessel permeability inside the scaffolds were measured by dynamic contrast enhanced (DCE) MR method using a gradient echo sequence at 4.7 T. MR images were acquired before and after intravenous administration of a T_1 contrast agent. The presence and viability of transplanted MSCs were assessed by bioluminescence imaging.

Accurate timing of transplantation steps is necessary, therefore in the next experiment, two time points for PIs transplantation were tested – 4 and 7 days after rod removal/MSCs transplantation. Here, bioluminescent PIs (1000 islets/animal) were transplanted into diabetic Lewis rats with or without 10 millions of MSCs (n = 6 in each group). Bioluminescence imaging was used to track viable transplanted islets. Vascularization in scaffolds was monitored by DCE MR and the histological analysis was performed at the end of the study. The weight and blood glucose levels of animals were measured at a regular basis.

4.2 Results and Discussion

Effect of MSCs on vascularization in scaffolds

In healthy animals with transplanted bioluminescent MSCs, DCE MR imaging confirmed **a positive effect of MSCs on vascularization and blood supply** in scaffolds; this effect was found also in diabetic rats with bioluminescent PIs transplanted together with non-bioluminescent MSCs. MR data analysis revealed a significantly higher area under the curve (AUC) (paired t-test; $p < 0.01$) in scaffolds supported with MSCs in comparison to scaffolds without MSCs indicating better vascularization. AUC value is dependent on vascular permeability and perfusion, which are related to vascularization. It has been already reported that MSCs secrete various pro-angiogenic substances, such as vascular endothelial growth factor (VEGF), which stimulates growth of the vascular network (Minteer et al. 2013). In our animal model, higher VEGF content in scaffolds with MSCs was confirmed by histology.

Tracking of pancreatic islets by bioluminescence imaging

Bioluminescent **PIs were tracked in scaffolds by bioluminescence imaging** for 4 months. Optical signals originating from the viable PIs remained stable for 120 days (Fig. 4).

Assessment of optimal timing of transplantation steps

DCE MR and bioluminescence imaging of scaffolds with bioluminescent MSCs revealed the **optimal window for further transplantation of PIs between day 3 and 9** after rod removal, when the optical signal reached its maximum and perfusion and vessel permeability inside the scaffold with MSCs started to elevate rapidly (Fig. 3).

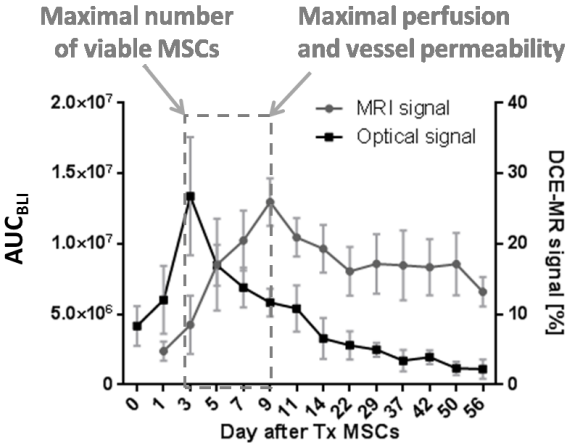

Fig. 3. The optimal time window for transplantation of PIs in scaffolds. The optimal condition in the artificial scaffolds by means of vascularization (assessed by DCE MR) and graft viability (assessed by bioluminescence imaging) was found between day 3 and 9 after rod removal/MSCs transplantation (Tx MSCs).

In the next step, multimodal imaging was applied for estimation of the optimal time for transplantation of PIs, concretely day 4 and day 7 after rod removal. In this experiment, bioluminescent PIs were transplanted with or without MSCs. The results of bioluminescence imaging showed that PIs transplanted **on day 4** after rod removal showed

higher optical signals (regardless of MSC presence) compared to transplantation on day 7 (paired t-test, p<0.0001) (Fig. 4).

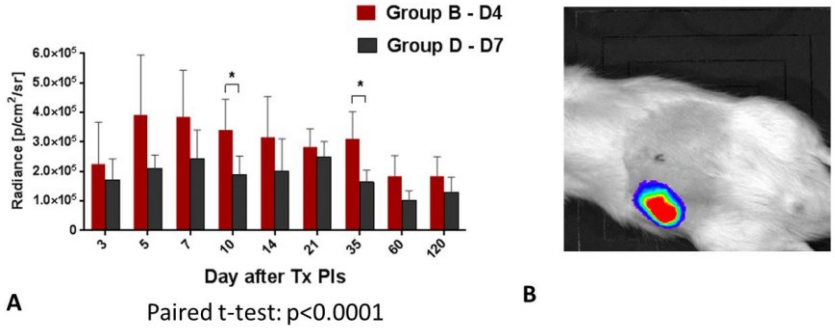

Fig. 4. *In vivo* bioluminescence imaging. Differences between optical signals originating from pancreatic islets transplanted on day 4 and day 7 after rod removal (A). D4 and D7 refer to the day after rod removal, unpaired t-test: *p < 0.05. A representative *in vivo* bioluminescence image of transplanted PIs in an artificial scaffold (B).

Similarly, DCE MR imaging confirmed statistically **higher AUCs** related to vascularization in the scaffolds with PIs and MSCs transplanted **on day 4** after rod removal compared to day 7 (paired t-test; p = 0.02) (Fig. 5).

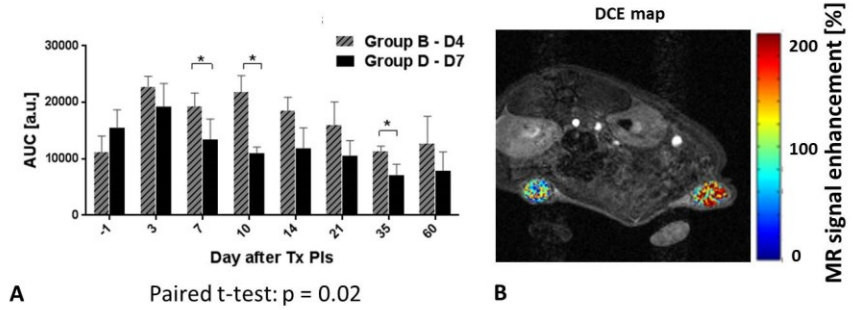

Fig. 5. DCE MR analysis related to vascularization. Differences in AUC between animal groups with PIs transplanted on days 4 (D4) and 7 (D7) after MSC transplantation (A). Unpaired t-test: * p < 0.05. A representative color-coded DCE map of a rat with transplanted scaffolds (B).

Similarly, quantitative histology analysis (CD31 staining against endothelial structures) showed **the highest microvascular density** (MVD) in scaffolds with PIs transplanted on day 4 after transplantation of MSCs. The results of MVD analysis strongly correlated with the results of DCE MR examination (AUC) ($R^2 = 0.99$).

An important result of the study was induction of **long-term normoglycemia** (for 4 months) in more than 80% of experimental animals. Viable grafts and insulin deposits were confirmed in scaffolds also by histology, which verified results obtained by other methods.

These findings confirm the efficiency of the model presented here for type 1 diabetes treatment. It is also worth noting that the transplanted mass was suboptimal and that the number of transplanted islets was lower compared to other scaffold models (Pepper et al. 2015; Pileggi et al. 2006), which is an important parameter for clinical application due to lack of donors.

The data were published in three publications in impacted journals (Gálisová, Fábryová, Sticová, et al. 2017; Gálisová, Fábryová, Jirák, et al. 2017; Fabryova et al. 2014).

5 Trimodal imaging platform for pancreatic islets

5.1 Materials and Methods

To precisely monitor transplanted PIs in scaffolds, isolated PIs were labeled with positively-charged multimodal nanoparticles based on poly(lactic-co-glycolic acid) (PLGA-NP) with encapsulated perfluoro-15-crown-5-ether and the near-infrared fluorescent dye indocyanine green. Labeling was accomplished by incubation of islets with 17 mg/mL of PLGA-NP within 24 hours (endocytosis).

After optimization of labeling procedure, 1000 and 3000 bioluminescent PIs labeled with PLGA-NP were transplanted into subcutaneous artificial scaffolds. The animals were monitored using *in vivo* ^{19}F MR, fluorescence and bioluminescence imaging in healthy Lewis rats for 2 weeks. The number of engrafted islets over time was assessed by ^{19}F MRI. Bioluminescence imaging served for assessment of viability of transplanted islets. A schematic illustration of the study design is shown in Fig. 6.

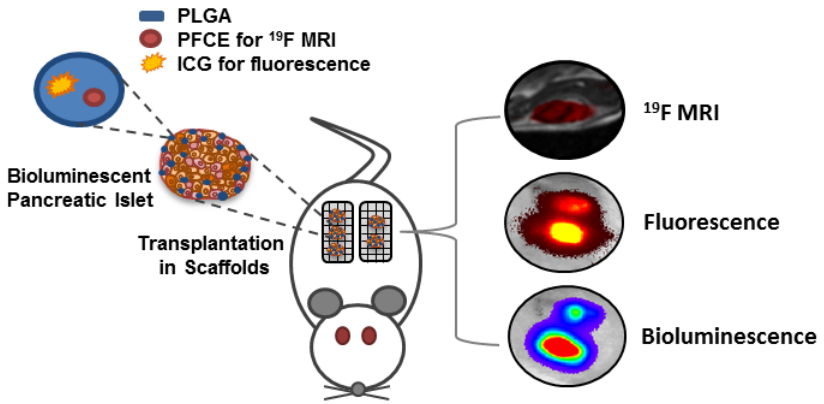

Fig. 6. Design of the experiment. Transplanted pancreatic islets labeled with multimodal PLGA-based nanoparticles were simultaneously visualized in artificial scaffolds by ^{19}F MR, fluorescence and bioluminescence imaging providing complementary information on graft localization, size and viability.

5.2 Results and Discussion

In this study, **a trimodal imaging platform** for *in vivo* examination of transplanted PIs by ^{19}F MR, bioluminescence and fluorescence imaging was introduced. Transplanted PIs were **unambiguously localized in the scaffolds by ^{19}F MRI**. Both 1000 and 3000 transplanted islets provided a detectable ^{19}F MR signal throughout the whole examination (14 days). The absolute signal revealed engraftment of an average of 2300 ± 200 and 1100 ± 300 islets in the scaffolds on day 1, corresponding to 3000 and 1000 transplanted islets respectively (manually counted prior to transplantation).

The maximum ^{19}F MR signal was detected on the first day after islet transplantation; after which the signal continuously declined (Fig. 7). The decrease of the ^{19}F MR signal to 44% on day 14 **corresponds with published experimental and clinical data** reporting a gradual loss of transplanted islets over 2 weeks after transplantation (Saudek et al. 2010; Jirák et al. 2009). To our knowledge, we supply **the first evidence of longitudinal tracking of transplanted islets by ^{19}F MRI *in vivo*.** Previous studies have visualized islets labeled by fluorine-containing probes at one time point post-transplantation only (Liang et al. 2017; Barnett et al. 2011). It should be noted that due to low sensitivity of ^{19}F MRI, long acquisition times (1 hour) were needed to visualize the transplanted grafts in our study.

The fluorescence signal originating from the labeled islets reached its maximum immediately after transplantation (day 1), then it rapidly decreased over the next week in all experimental groups. This result revealed **instability of the fluorescent dye** and its limited applicability for longitudinal *in vivo* studies.

In vivo BLI confirmed the presence of **viable transplanted islets** in the scaffolds throughout the entire 14 day-experiment. Labeling with nanoparticles did not impair the viability or survival of transplanted islets measured by *in vivo* bioluminescence, as the labeled islets provided a similar bioluminescence signal compared to unlabeled controls. Importantly, insulin deposits were present at the same locations

as luciferase within the graft (Fig. 8) confirming **functionality of bioluminescent islets**.

The ^{19}F MR signal strongly correlated with bioluminescence between days 4 and 14 (R^2 = 0.99) indicating **the fast clearance** of PLGA-NPs from the transplantation site, which addresses one of the major issues with intracellular imaging labels because the cleared nanoparticles do not contribute to the false positive data after cell death. Therefore, the proposed PLGA-NP platform is reliable for reflecting the status of transplanted PIs *in vivo*.

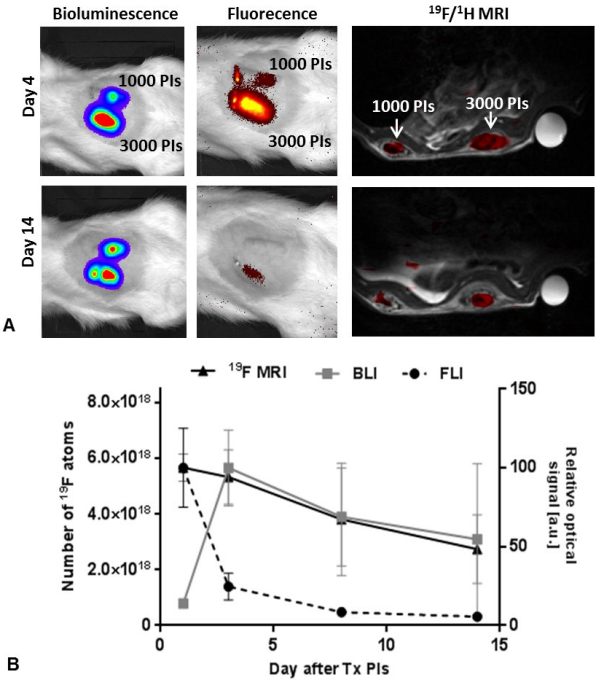

Fig. 7. Trimodal imaging of transplanted pancreatic islets in scaffolds. Representative bioluminescence, fluorescence and axial $^{19}F/^{1}H$ MR images of 1000 and 3000 pancreatic islets transplanted into scaffolds on days 4 and 14 (A). Time course of bioluminescence (BLI), fluorescence (FLI) and ^{19}F MRI signals for 3000 labeled transplanted islets. MRI signal is recalculated to the corresponding number of ^{19}F nuclei (left axis); the optical signals (BLI, FLI) are normalized to the maximum value (=100 %, right axis).

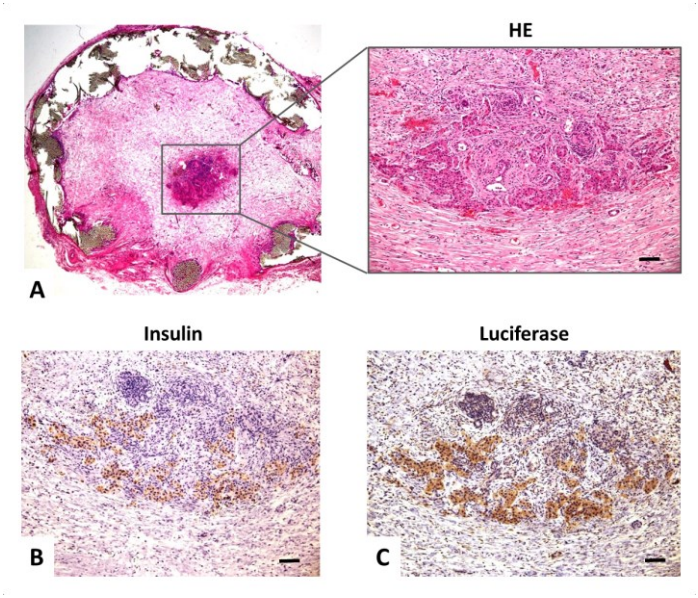

Fig. 8. Histology of scaffolds on day 14 after islet transplantation. The representative images of transplanted islets in a scaffold stained with haematoxylin and eosin (left magnification 20×) (A). A detail of the viable graft is shown at higher magnification on right. Immunohistochemical staining with the primary antibodies, anti-insulin (B) and anti-luciferase (C). Insulin- and luciferase-positive cells were present at the same locations within the graft. The scale bar corresponds to 100 μm.

6 Conclusion

In this thesis, novel imaging approaches for visualization of pancreatic islets were tested with the intention to improve the detection of islets after their transplantation.

CEST as a frequency-selective approach has a great potential for MR imaging; however our results pointed out to low sensitivity of the method for cell imaging and high toxicity of the tested CEST probes. Therefore, the use of the CEST agents as exogenous labels for PIs and their *in vivo* application is at current instrumental setting inappropriate.

Multimodal imaging with bioluminescence and MR imaging was used for optimization of a transplantation protocol at an alternative transplant site – artificial scaffolds. Transplantation of a suboptimal PIs mass on day 4 after rod removal from scaffolds was found to be superior in comparison to day 7 due to higher islet viability and vascularization. Using optimized protocol, long-term normoglycemia was induced in more than 80% of experimental animals, therefore the model holds a potential for further clinical applications.

Three imaging modalities, including specific ^{19}F MRI and sensitive optical imaging were applied for monitoring of transplanted PIs using the optimized transplantation protocol. Multimodal probes can provide complementary information about distribution and viability of transplanted grafts. The bioluminescence signal correlated with the ^{19}F MR signal indicating clearance of PLGA-NPs from the transplantation site after cell death eliminating false positive data. This result addresses one of the major issues of intracellular imaging labels. The proposed imaging platform is therefore reliable for quantification of survived transplanted islets.

The work contributes to the improvement of transplantation protocol for pancreatic islets and may help to monitor non-invasively the distribution and viability of transplanted islets or processes causing rejection. Moreover, multimodal imaging might speed up translation of these alternative transplant models into clinical practice.

7 References

Barnett, B.P. et al., 2011. Use of perfluorocarbon nanoparticles for non-invasive multimodal cell tracking of human pancreatic islets. *Contrast Media Mol Imaging*, 6(4), pp.251–259.

Fabryova, E. et al., 2014. Effect of mesenchymal stem cells on the vascularization of the artificial site for islet transplantation in rats. *Transplantation proceedings*, 46(6), pp.1963–6.

Gálisová, A. et al., 2016. Magnetic Resonance Visualization of Pancreatic Islets Labeled by PARACEST Contrast Agents at 4.7 T. *Journal of Molecular Imaging & Dynamics*, 6(1), pp.4–10.

Gálisová, A., Fábryová, E., Jirák, D., et al., 2017. Multimodal Imaging Reveals Improvement of Blood Supply to an Artificial Cell Transplant Site Induced by Bioluminescent Mesenchymal Stem Cells. *Molecular Imaging and Biology*, 19(1), pp.15–23.

Gálisová, A., Fábryová, E., Sticová, E., et al., 2017. The Optimal Timing for Pancreatic Islet Transplantation into Subcutaneous Scaffolds Assessed by Multimodal Imaging. *Contrast Media and Molecular Imaging*, p.5418495.

Jirák, D. et al., 2009. Monitoring the survival of islet transplants by MRI using a novel technique for their automated detection and quantification. *Magnetic Resonance Materials in Physics, Biology and Medicine*, 22(4), pp.257–65.

Jirák, D. et al., 2004. MRI of transplanted pancreatic islets. *Magnetic resonance in medicine*, 52(6), pp.1228–33.

Kim, J., Kalimuthu, S. & Ahn, B., 2015. In vivo cell tracking with bioluminescence imaging. *Nuclear Medicine and Molecular Imaging*, 49(1), pp.3–10.

Krchová, T. et al., 2013. Lanthanide(III) complexes of aminoethyl-DO3A as PARACEST contrast agents based on decoordination of the weakly bound amino group. *Dalton transactions*, 42(44), pp.15735–47.

Krchová, T. et al., 2016. Ln(III)-complexes of a DOTA analogue with an ethylenediamine pendant arm as pH-responsive PARACEST contrast agents. *Dalton Transactions*, 45(8), pp.3486–3496.

Liang, S. et al., 2017. Comparison of different compressed sensing algorithms for low SNR 19F MRI applications — Imaging of transplanted pancreatic islets and cells labeled with perfluorocarbons. *NMR in Biomedicine*, 30(11), p.e3776.

Minteer, D., Marra, K. & Rubin, J., 2013. Adipose-derived mesenchymal stem cells: biology and potential applications. *Adv Biochem Eng Biotechnol*, 129, pp.59–71.

Nicholls, F.J. et al., 2015. Simultaneous MR imaging for tissue engineering in a rat model of stroke. *Scientific reports*, 5, p.14597.

Pepper, A.R. et al., 2015. Diabetes Is Reversed in a Murine Model by Marginal Mass Syngeneic Islet Transplantation Using a Subcutaneous Cell Pouch Device. *Transplantation*, 99(11), pp.2294–300.

Pileggi, A. et al., 2006. Reversal of diabetes by pancreatic islet transplantation into a subcutaneous, neovascularized device. *Transplantation*, 81(9), pp.1318–24.

Saudek, F. et al., 2010. Magnetic Resonance Imaging of Pancreatic Islets Transplanted Into the Liver in Humans. *Transplantation*, 90(12), pp.1602–1606.

Shapiro, J.A. et al., 2006. International Trial of the Edmonton Protocol for Islet Transplantation. *The New England journal of medicine*, 355, pp.1318–1330.

Srinivas, M. et al., 2012. Labeling cells for in vivo tracking using (19)F MRI. *Biomaterials*, 33(34), pp.8830–40.

Ward, K.M., Aletras, A.H. & Balaban, R.S., 2000. A new class of contrast agents for MRI based on proton chemical exchange dependent saturation transfer (CEST). *Journal of magnetic resonance*, 143(1), pp.79–87.

8 List of publications

8.1 Publications related to the thesis

(1) **Gálisová A**, Jirák D, Krchová T, Herynek V, Fábryová E, Kotek J, Hájek M. Magnetic resonance visualization of pancreatic islets labeled by PARACEST contrast agents at 4.7 T. *Journal of Molecular Imaging and Dynamics 2016*; 6:121. **IF: 2**

(2) Fabryova E, Jirak D, Girman P, Zacharova K, **Galisova A**, Saudek F, Kriz J. Effect of Mesenchymal Stem Cells on the Vascularization of the Artificial Site for Islet Transplantation in Rats. *Transplantation Proceeding 2014*; 46:1963-1966. **IF: 0.9**

(3) **Gálisová A**, Fábryová E, Jirák D, Sticová E, Lodererová A, Herynek V, Kříž J, Hájek M. Multimodal imaging reveals improvement of blood supply to an artificial cell transplant site induced by bioluminescent mesenchymal stem cells. *Molecular Imaging and Biology 2017*; 19(1):15-23. **IF: 3.5**

(4) Krchová T, **Gálisová A**, Jirák D, Hermann P, Kotek J. Ln(III)-complexes of a DOTA analogue with an ethylenediamine pendant arm as pH-responsive PARACEST contrast agents. *Dalton Transactions 2016*; 45(8):3486-96. **IF: 4.0**

(5) **Gálisová A**, Fábryová E, Sticová E, Kosinová L, Jirátová M, Herynek V, Berková Z, Kříž J, Hájek M, Jirák D. The optimal timing for pancreatic islet transplantation into subcutaneous scaffolds assessed by multimodal imaging. *Contrast Media and Molecular Imaging 2017*. Article ID 5418495. **IF: 3.3**

(6) Herynek V, **Gálisová A**, Srinivas M, van Dinther EAW, Kosinová L, Ruzicka J, Jirátová M, Kriz J, Jirák D. Pre-Microporation Improves Outcome of Pancreatic Islet Labeling for Optical and ^{19}F MR Imaging. *Biological Procedures Online 2017*; 19:6. **IF: 2.0**

(7) **Gálisová A**, Herynek V, Srinivas M, Swider E, Sticová E, Kosinová L, Pátiková A, Kříž J, Hájek M, Jirák D. A novel trimodal platform for tracking of transplanted pancreatic islets: ^{19}F MR, fluorescence and bioluminescence imaging. Submitted to *Molecular Imaging and Biology* (April 2018). **IF: 3.5**

8.2 Other publications

(1) **Gálisová A**, Bačiak L, Jozefovičová M, Kukurova J I, Kebis A, Ambrusova K, Dubovicky M, Estera, Sadlonova I, Kronnerwetter C, Berg A, Krssak M, Kasparova S. Pathophysiological rat model of vascular dementia: magnetic resonance spectroscopy, microimaging and behavioral study. *Brain Research 2014*; 1568:10-20. **IF: 2.8**

(2) Blahut J, Hermann P, **Gálisová A**, Herynek V, Cisarova I, Tošner Z, Kotek J. Nickel(II) complexes of N–CH2CF3 cyclam derivatives as contrast agents for 19F magnetic resonance imaging. *Dalton Transactions 2016*; 45,474-478. **IF: 4.0**

(3) Blahut J, Bernášek K, **Gálisová A**, Herynek V, Císařová I, Kotek J, Lang J, Matějková S, Hermann P. Paramagnetic 19F Relaxation Enhancement in Nickel(II) Complexes of N‑Trifluoroethyl Cyclam Derivatives and Cell Labeling for 19F MRI. *Inorganic Chemistry 2017*; 56:13337-13348. **IF: 4.9**

(4) Krchová T, Herynek V, **Gálisová A**, Blahut J, Hermann P, Kotek J. Eu(III) Complex with DO3A-amino-phosphonate Ligand as a Concentration-Independent pH-Responsive Contrast Agent for Magnetic Resonance Spectroscopy (MRS). *Inorganic Chemistry 2017*; 56 (4), 2078–2091. **IF: 4.9**

(5) Šmejkalová D, Nešporová K, Huerta-Angeles G, Syrovátka J, Jirák D, **Gálisová A**, Velebný V. Selective In Vitro Anticancer Effect of Superparamagnetic Iron Oxide Nanoparticles Loaded in Hyaluronan Polymeric Micelles. *Biomacromolecules 2014*. **IF: 5.2**

(6) Herynek V, Turnovcová K, Veverka P, Dědourková T, Žvátora P, Jendelová P, **Gálisová A**, Kosinová L, Jiráková K, Syková E. Using ferromagnetic nanoparticles with low Curie temperature for magnetic resonance imaging-guided thermoablation. *International Journal of Nanomedicine 2016*; 11:3801-3811. **IF: 4.4**

(7) Jirátová M, Pospíšilová A, Rabyk M, Pařízek M, Kovář J, **Gálisová A**, Hrubý M, Jirák D. Biological characterization of a novel hybrid copolymer carrier system based on glycogen. *Drug Delivery and Translation Research 2018*; 8(1):73-82. **IF: 3.1**

(8) Rabyk M, **Galisova A**, Jiratova M, Patsula V, Srbova L, Loukotova L, Jirak D, Stepanek P, Hruby M. Mannan-based conjugates as multimodal imaging platform for sentinel lymph nodes. *Journal of Materials Chemistry B 2018*. **IF: 4.5**

(9) Šedivý P, Herynek V, Dezortová M, Drobný M, **Gálisová A**, Hájek M. ^{31}P and ^{19}F MR spectroscopy and imaging in IKEM. *Česká radiologie 2017*; 71(4):312-322. **no IF**